

## Modelling concentration fluctuation moments for spherically symmetric mean concentration<sup>(\*)</sup>

N. MOLE, E. D. CLARKE and E. RIETZLER

*School of Mathematics and Statistics, University of Sheffield  
Hicks Building, Sheffield S3 7RH, U.K.*

(ricevuto il 10 Gennaio 1996; revisionato il 26 Agosto 1996; approvato il 23 Settembre 1996)

**Summary.** — Clarke and Mole (*Environmetrics*, **6** (1995) 607-617) presented a model for concentration fluctuation moments of a passive scalar dispersing in a turbulent flow. This followed Sullivan and Moseley's work in making use of the equation for the evolution of the concentration moments integrated over all space, together with Chatwin and Sullivan's (*J. Fluid Mech.*, **212** (1990) 533-556) description relating higher moments to the mean concentration. The model incorporated a simple closure to express the concentration gradient in terms of the concentration. Numerical results were presented for 1, 2 and 3 spatial dimensions under the assumption that the spatial distribution of the mean concentration was spherically symmetric and Gaussian. Two simple functional forms were used for the spreading rate of the mean cloud. Here those results are briefly summarised. Some asymptotic large time results are also given for spherically symmetric mean concentration of general functional form, and numerical results are obtained for a number of different functional forms.

PACS 92.60.Ek – Convection, turbulence and diffusion.

PACS 47.27 – Turbulent flows, convection, and heat transfer.

PACS 01.30.Cc – Conference proceedings.

### 1. – Introduction

The concentration of a passive scalar dispersing in a turbulent flow is a random variable. A proper description of such dispersion must include not only the mean concentration, but also the distribution of the concentration fluctuations about the mean. Here we

---

(\*) Paper presented at EUROMECH Colloquium 338 "Atmospheric Turbulence and Dispersion in Complex Terrain" and ERCOFTAC Workshop "Data on Turbulence and Dispersion in Complex Atmospheric Flows", Bologna, 4-7 September 1995.

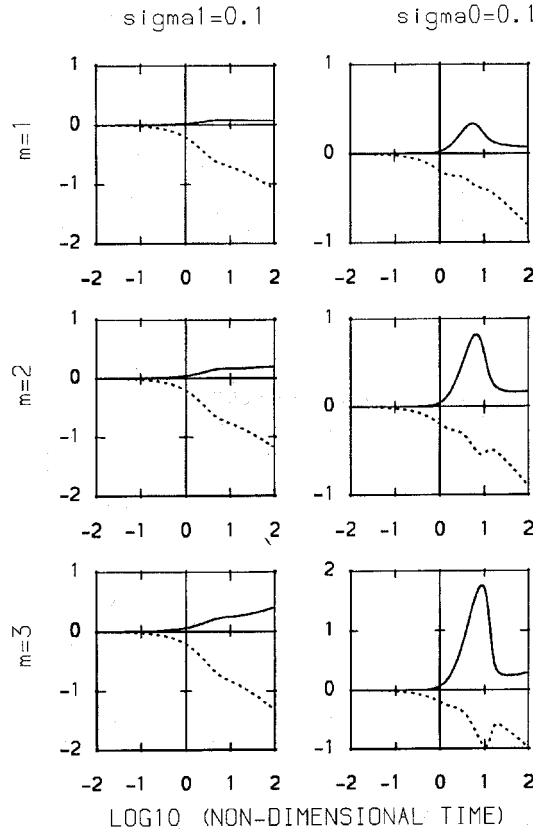


Fig. 1. – Evolution of  $\log_{10}\alpha$  (solid line) and  $\log_{10}\beta$  (dashed line) in non-dimensional time  $\log_{10}\tau$ . Results are shown for 1, 2 and 3 spatial dimensions, and for  $\Sigma_1 = \Sigma_0 = 0.1$ .

shall concentrate on modelling concentration fluctuation moments, since these are characteristics of the distribution which can be modelled relatively conveniently from the underlying physical equations. Models for the probability density function (PDF) of concentration can be constructed from the moments.

Chatwin and Sullivan [1] addressed the problem of dispersing passive scalars released from a source of uniform concentration in self-similar turbulent flows. They postulated that the mean concentration  $\mu = E\{\Gamma\}$ , the variance of concentration  $\sigma^2 = E\{(\Gamma - \mu)^2\}$  and the higher moments of concentration  $E\{(\Gamma - \mu)^n\}$  satisfied, to a good approximation, the following relationships:

$$(1) \quad \sigma^2 = \beta^2 \mu (\alpha \mu_0 - \mu),$$

$$(2) \quad \frac{E\{(\Gamma - \mu)^n\}}{\mu_0^n} = A_n \frac{\beta^n}{\alpha} \left[ \frac{\mu}{\mu_0} \left( \alpha - \frac{\mu}{\mu_0} \right)^n + (-1)^n \left( \alpha - \frac{\mu}{\mu_0} \right) \left( \frac{\mu}{\mu_0} \right)^n \right].$$

Here  $\alpha$ ,  $\beta$  and  $A_n$  are parameters and  $\mu_0$  is a local scale for  $\mu$  (*e.g.* the largest value of  $\mu$  in a cross-section). To make physical sense we must have  $\alpha \geq 1$ , and  $\beta$  and  $A_n$  non-negative. Chatwin and Sullivan [1] presented experimental evidence in support of (1) and

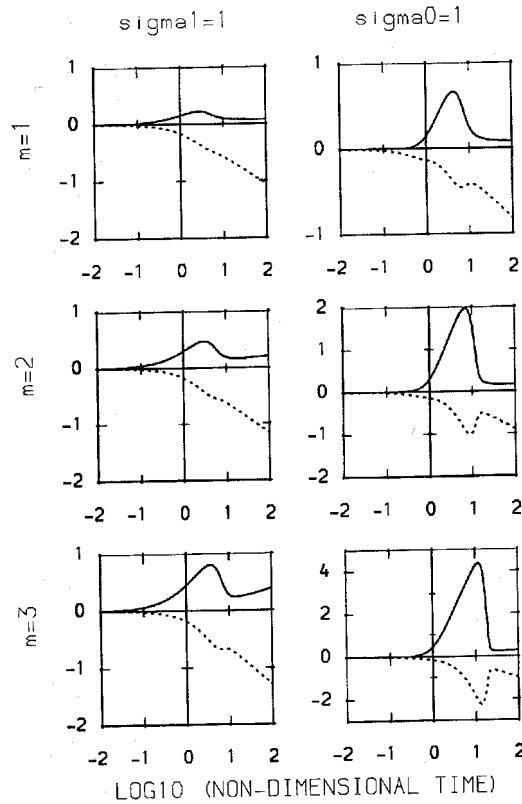


Fig. 2. - As fig. 1 but  $\Sigma_1 = \Sigma_0 = 1$ .

(2), and more support has subsequently emerged (Sullivan and Yip [2], Chatwin *et al.* [3], Moseley [4], Sawford and Sullivan [5]), including for some non-self-similar flows. Sawford and Sullivan [5] considered non-uniform sources, in particular a Gaussian source, and concluded that, except close to the source or soon after release, only minor modifications to (1) and (2) are required. Sullivan and Moseley constructed a model (described in Moseley [4]) for the evolution of  $\alpha$  and  $\beta$ . This was based on the following equation (see Chatwin and Sullivan [6]):

$$(3) \quad \frac{\partial}{\partial t} \int E \{ \Gamma^n \} dV = -n(n-1)\kappa \int E \{ \Gamma^{n-2} (\nabla \Gamma)^2 \} dV,$$

for  $n \geq 2$ , where the integrals are taken over all space and  $\kappa$  is the molecular diffusivity. Equation (3) holds exactly if  $\Gamma = o(|\mathbf{x}|^{-(m-1)/n})$  in unbounded regions, where  $m$  is the number of spatial dimensions. To obtain equations for the evolution of  $\alpha$  and  $\beta$ , (3) was combined with (1) and (2) for  $n = 3$ , using the closure assumption

$$(4) \quad (\nabla \Gamma)^2 = B \left( \frac{\Gamma - \mu}{\lambda} \right)^2.$$

Here  $\lambda$  is the conduction cut-off and  $B$  is a constant.

Chatwin and Sullivan [1] suggested that  $A_n^{1/n}$  is  $O(1)$ , so for simplicity  $A_3$  was taken to be 1.

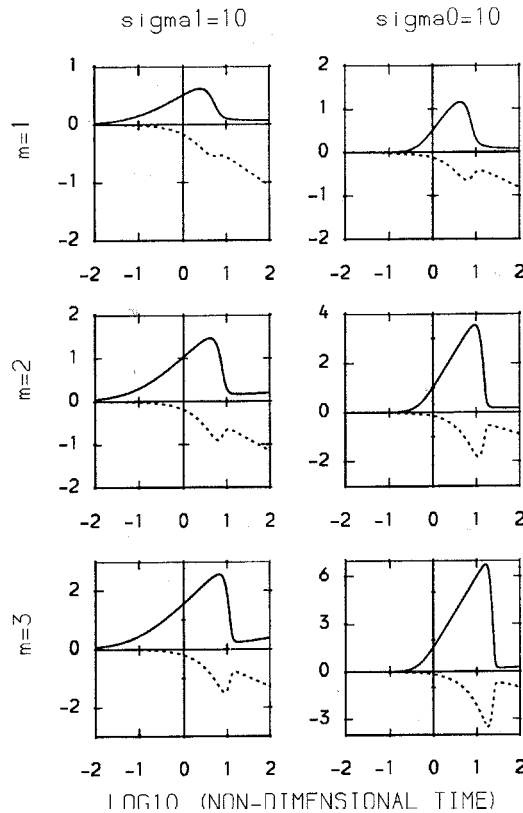


Fig. 3. - As fig. 1 but  $\Sigma_1 = \Sigma_0 = 10$ .

The model required  $\mu(x, t)$  as an input—a Gaussian spatial distribution with prescribed spreading rate was assumed. Mole [7] gives a more detailed outline of this model.

When restricted to 1 spatial dimension (corresponding to a continuous line source in real three-dimensional space, with the temporal evolution in the model converted to a downwind evolution through the relation  $X = Ut$ , where  $X$  is the downwind distance from the source and  $U$  is the mean velocity) this model generally predicted a rise in  $\alpha$  from its initial value of 1 to a maximum, and a subsequent decrease to a value between 1 and 2. However, in 2 and 3 spatial dimensions (corresponding to a continuous point source and to an instantaneous release, respectively, in real space) it gave the unphysical result  $\alpha < 1$  (implying negative variance at the cloud centre from (1)), and breakdown of the numerical solutions. Clarke and Mole [8] showed the latter to be associated with a singularity in the evolution equations for  $\alpha$  and  $\beta$ , and overcame both these problems by using the following closure, instead of (4):

$$(5) \quad \frac{\lambda^2}{B} E \{ \Gamma^{n-2} (\nabla \Gamma)^2 \} = \frac{1}{2} E \{ \Gamma^{n-2} (\Gamma - \mu)^2 \} + \frac{1}{2} E \{ \Gamma^{n-2} \} E \{ (\Gamma - \mu)^2 \}.$$

Clarke and Mole [8] showed that this closure (and (4) also) fitted some atmospheric boundary layer data reasonably well, with  $\lambda/\sqrt{B}$  approximately in the range 0.3–0.5 m (but note that this does not guarantee that a model incorporating these closures will produce a good fit to experimental data, or even give physically sensible solutions).

**2. – Numerical results for Gaussian mean concentration**

Clarke and Mole [8] assumed (following Moseley [4]) that the mean concentration had a Gaussian spatial distribution with width  $L$

$$\mu(\mathbf{x}, t) = \mu_0(t)e^{-\frac{1}{2}\left(\frac{|\mathbf{x}|}{L}\right)^2},$$

where  $L$  was defined by

$$\left(\frac{L}{L_0}\right)^2 = 1 + \Sigma_0\tau^3,$$

the inertial subrange relative dispersion result for intermediate times (Batchelor [9]), or by the large time result for absolute dispersion in homogeneous turbulence (Batchelor [10])

$$\left(\frac{L}{L_0}\right)^2 = 1 + \Sigma_1\tau.$$

$L_0$  is the source width and  $\tau = 2B\kappa t/\lambda^2$  is the non-dimensional time. Experimental evidence in many cases (*e.g.* Becker *et al.* [11], Birch *et al.* [12], Gad-el Hak and Morton [13]) supports the Gaussian form for the mean concentration some time after release.

The initial conditions suitable for modelling a source of uniform concentration are  $\alpha = 1$ ,  $\beta = 1$ . For more discussion of initial conditions, and of the appropriateness of modelling a uniform source with Gaussian  $\mu$ , see Mole [7].

This model then applies to the case of uniform flow in an unbounded fluid, with an idealised form for  $\mu(\mathbf{x}, t)$ . However, (3) is satisfied in the presence of solid boundaries, and the available evidence suggests that (1) and (2) apply to more general flows such as boundary layers and jets. Therefore, to apply the model to these more realistic cases may only require the use of a realistic model for  $\mu(\mathbf{x}, t)$  (possibly with minor changes to the closure scheme). This would also avoid any problems associated with using Gaussian mean for a uniform source. The use of more general forms for  $\mu(\mathbf{x}, t)$  is discussed in the following sections.

Figures 1-3 show the evolution of  $\alpha$  and  $\beta$  using this model, for  $\Sigma_1, \Sigma_0 = 0.1, 1, 10$ . In nearly all cases  $\alpha$  increases, reaches a peak (in all cases shown this is for  $\tau$  less than 20) and then decreases, in all cases reaching a value between 1 and 2 before  $\tau = 50$ . ( $\alpha = 2$  is significant in that for  $\alpha < 2$  the variance attains its peak off the centreline, and the centreline skewness is negative. For  $\alpha > 2$  the variance is largest on the centreline, and the centreline skewness is positive.) The exceptions are  $m = 2, 3$  for  $\Sigma_1 = 0.1$ , when  $\alpha$  increases monotonically.  $\beta$  decreases towards zero, often with a subsidiary maximum. The peaks in  $\alpha$  are larger and later for higher dimensions, and for  $\Sigma_0$  as opposed to  $\Sigma_1$ , and also for larger  $\Sigma$  values. (The only exception to this is that in 1 dimension the peak is earlier for larger  $\Sigma$  values.) The larger  $\alpha$  is, the smaller  $\beta$  tends to be.

The largest value of  $\alpha$  shown in figs. 1-3 is about  $5.3 \times 10^6$  (for  $\Sigma_0 = 10, m = 3$ ). While values of  $\alpha$  so far observed are all  $O(1)$ , it is not clear that large values can be ruled out. In the model the concentration moments remain finite even if  $\alpha \rightarrow \infty$ . Large values of  $\alpha$  correspond to a linear rather than quadratic relationship between the variance and the mean (see eq. (1)). Furthermore, it has not yet even been tested experimentally whether the  $\alpha - \beta$  formulation holds for  $m = 3$  (because of the greater difficulty in making the required measurements), so observed  $\alpha$  values are not available. Also,  $\Sigma_0 = 10$  is

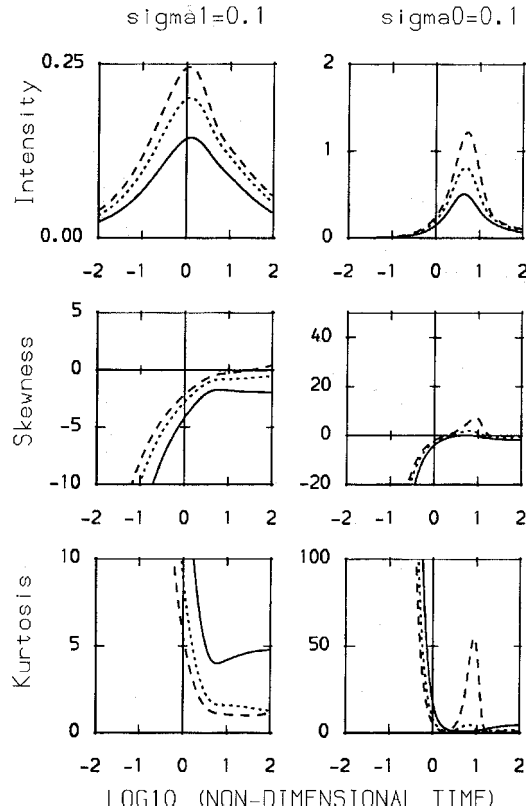


Fig. 4. – Evolution of centreline intensity, skewness and kurtosis in non-dimensional time  $\log_{10} \tau$ . Results are shown for  $m = 1$  (solid lines),  $m = 2$  (short dashes) and  $m = 3$  (long dashes), and for  $\Sigma_1 = \Sigma_0 = 0.1$ .

probably unrealistic. For  $\Sigma_1 = 1$  the largest value of  $\alpha$  achieved is about 6, which is certainly consistent with observation.

Figures 4-6 show the corresponding evolution of centreline intensity  $I (= \beta(\alpha-1)^{1/2})$ , skewness  $S (= (\alpha-2)(\alpha-1)^{-1/2})$  and kurtosis  $K (= S^2 + 1, \text{ if we take } A_4 = 1, \text{ see Mole and Clarke [14])}$ . As  $\tau \rightarrow 0$ ,  $I \rightarrow 0$ ,  $S \rightarrow -\infty$  and  $K \rightarrow \infty$ . With increasing  $\tau$ ,  $I$  increases to a maximum and then decays to zero as the variance is dissipated, while  $S$  increases rapidly (the more so the greater  $\Sigma$ ). For rapidly spreading clouds (large  $\Sigma$  and  $m$ )  $\alpha$ , and hence  $S$  also, reaches large values before declining again. For all  $\Sigma$  values so far explored,  $\alpha$  drops below 2 and  $S$  becomes negative again. If cloud spread is sufficiently slow (for the cases shown this is for  $\Sigma_1 = 0.1$  with  $m = 1, 2$ , and  $\Sigma_1 = 1$  with  $m = 1$ ) then  $\alpha$  never exceeds 2 and  $S$  is always negative.

### 3. – Large time behaviour

Suppose that the mean concentration is spherically symmetric, with the same functional form for all time. We can then write, in centre-of-mass coordinates,

$$\mu(\mathbf{x}, \tau) = \mu_0(\tau)g(s),$$

where  $s = |\mathbf{x}|^2/2L^2$ . Thus the Gaussian form used above has  $g(s) = e^{-s}$ .

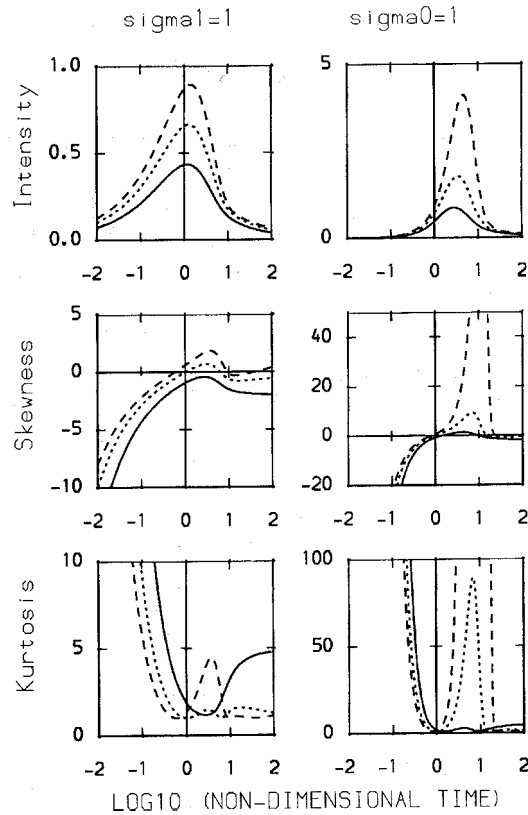


Fig. 5. – As fig. 4 but  $\Sigma_1 = \Sigma_0 = 1$ .

Let

$$Q_n = \int \mu^n dV = \mu_0^n \int g^n(s) dV$$

and  $Q = Q_1$  ( $Q$  is a constant—the amount of pollutant released). In general the evolution of  $\alpha$  and  $\beta$  in the model depends on  $\dot{Q}_2$  and  $\dot{Q}_3$ , where  $\dot{\phantom{x}}$  denotes  $\frac{d}{d\tau}$ . However, in the spherically symmetric case this reduces to a dependence on  $\dot{L}/L$ , as shown below.

In spherical polar coordinates  $(r, \theta, \phi)$  we have

$$dV = \begin{cases} 2dr = 2L(2s)^{-1/2} ds, & m = 1, \\ r dr d\phi = L^2 ds d\phi, & m = 2, \\ r^2 \sin \theta dr d\theta d\phi = L^3(2s)^{1/2} \sin \theta ds d\theta d\phi, & m = 3, \end{cases}$$

where  $m$  is the number of spatial dimensions in the model. Therefore

$$Q_n = a_m I_n L^m \mu_0^n,$$

where  $a_1 = \sqrt{2}$ ,  $a_2 = 2\pi$ ,  $a_3 = 4\sqrt{2}\pi$  and

$$I_n = \int_0^\infty s^{\frac{1}{2}m-1} g^n(s) ds.$$

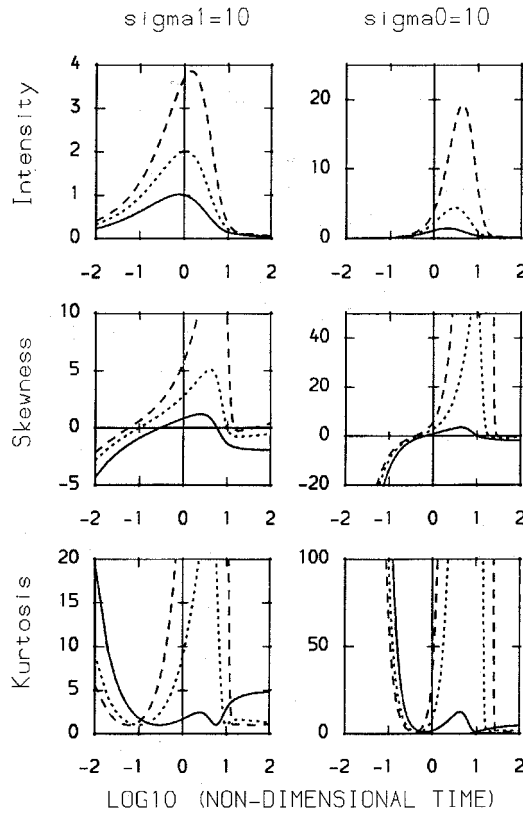


Fig. 6. - As fig. 4 but  $\Sigma_1 = \Sigma_0 = 10$ .

The  $I_n$  are constants determined by the function  $g$ . Thus

$$\dot{Q}_n = \left( \frac{m\dot{L}}{L} + \frac{n\dot{\mu}_0}{\mu_0} \right) Q_n.$$

Since  $Q_1 = Q$  is a constant,  $\dot{\mu}_0/\mu_0 = -m\dot{L}/L$  so

$$\frac{\dot{Q}_n}{Q_n} = -(n-1)m\frac{\dot{L}}{L}.$$

If we let

$$\hat{Q}_n = \frac{Q_n}{\mu_0^{n-1}Q} = \frac{I_n}{I_1},$$

then the evolution equations for  $\alpha$  and  $\beta$  are

$$\begin{aligned} \frac{D\dot{\alpha}}{\beta} &= -\frac{m\dot{L}}{L} \left[ 2\alpha(1-\beta)(2+2\beta-\beta^2)\hat{Q}_3 - \alpha^2\beta(3-6\beta+4\beta^2)\hat{Q}_2 + \right. \\ &\quad \left. + \alpha^3\beta^3 + 2(1-\beta)^3\hat{Q}_2\hat{Q}_3 - 3\alpha(1-\beta)(2-\beta+\beta^2)\hat{Q}_2^2 \right], \\ \frac{D\dot{\beta}}{\beta^2} &= \frac{1}{2}\alpha\beta^3(\alpha - \hat{Q}_2) + 3\beta^2(1-\beta)(\hat{Q}_3 - \hat{Q}_2^2) - \\ &\quad - \frac{m\dot{L}}{L}(1-\beta) \left[ \alpha\beta(2-\beta)\hat{Q}_2 + (1-\beta) \left\{ 3(1+\beta)\hat{Q}_2^2 - 2(1+2\beta)\hat{Q}_3 \right\} \right], \end{aligned}$$



where  $D$  is defined by

$$\frac{D}{\beta^3} = -\alpha\beta(\alpha - \hat{Q}_2) - 6(1 - \beta)(\hat{Q}_3 - \hat{Q}_2^2).$$

Thus the evolution of  $\alpha$  and  $\beta$  is completely determined by  $\dot{L}/L$ ,  $\hat{Q}_2$  and  $\hat{Q}_3$ . Mole [7] showed that  $\beta \rightarrow 0$  as  $\tau \rightarrow \infty$ , so at large time there is an approximately stationary state  $\alpha = \alpha_S$ , where

$$\alpha_S = \frac{\hat{Q}_2\hat{Q}_3}{3\hat{Q}_2^2 - 2\hat{Q}_3} = \frac{I_2I_3}{3I_2^2 - 2I_1I_3}.$$

While  $\alpha_S$  can take unphysical negative values, it turns out that  $\alpha$  cannot attain such negative values at large time. It can be shown (paper currently in preparation) that as  $\tau \rightarrow \infty$

$$\alpha \rightarrow \begin{cases} \alpha_S, & \alpha_S > \hat{Q}_2, \\ \infty, & \alpha_S < -\hat{Q}_2. \end{cases}$$

(Note that it is not possible for  $-\hat{Q}_2 < \alpha_S < \hat{Q}_2$ —see appendix A.) This result is independent of the form of  $\dot{L}/L$ .

For the Gaussian form  $g(s) = e^{-s}$  we have

$$I_n = \begin{cases} (\pi/n)^{1/2}, & m = 1, \\ 1/n, & m = 2, \\ (\pi/4n^3)^{1/2}, & m = 3, \end{cases}$$

so  $\hat{Q}_n = n^{-m/2}$  and

$$\alpha_S = \begin{cases} \frac{\sqrt{2}}{3\sqrt{3}-4} \approx 1.182, & m = 1, \\ 2, & m = 2, \\ \frac{2\sqrt{2}}{9\sqrt{3}-16} \approx -6.873, & m = 3. \end{cases}$$

These results are supported by the numerical integrations. Correspondingly, centreline skewness tends to a limit  $S_\infty$ , where

$$S_\infty = \begin{cases} -1.915, & m = 1, \\ 0, & m = 2, \\ \infty, & m = 3. \end{cases}$$

The corresponding limits for  $K$  are 4.668, 1 and  $\infty$ . However, these limits are approached extremely slowly, so it is not clear how much relevance they have to problems of practical interest.

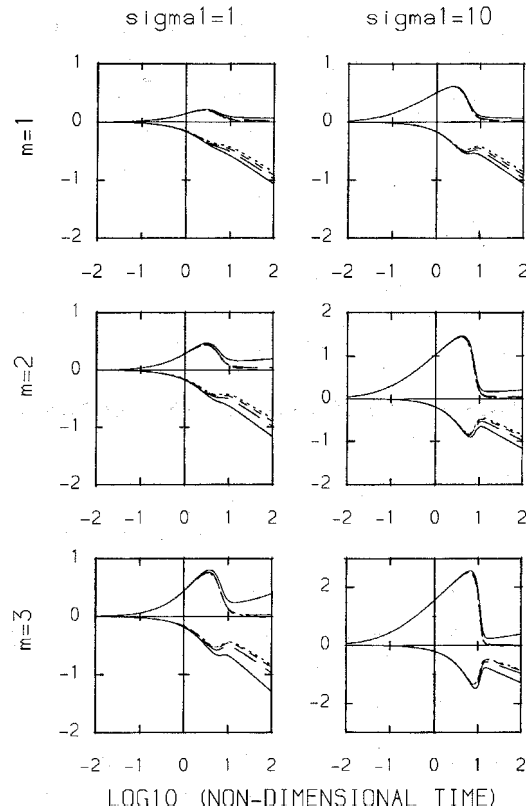


Fig. 7. – Evolution of  $\log_{10}\alpha$  (upper curves) and  $\log_{10}\beta$  (lower curves) in non-dimensional time  $\log_{10}\tau$ , with Gaussian mean  $g(\phi) = e^{-\phi}$  (solid line),  $g(\phi) = g_1(\phi)$  (short dashes),  $g(\phi) = g_3(\phi)$  (medium dashes),  $g(\phi) = g_5(\phi)$  (long dashes). Results are shown for 1, 2 and 3 spatial dimensions, and for  $\Sigma_1 = 1$  and 10.

#### 4. – Effect of differences in the mean

Figure 7 compares the previous results for  $\alpha$  and  $\beta$  with those using the following polynomial approximations to the Gaussian:

$$g_1(s) = 1 - s,$$

$$g_3(s) = 1 - s + \frac{1}{2}s^2 - \frac{1}{6}s^3,$$

$$g_5(s) = 1 - s + \frac{1}{2}s^2 - \frac{1}{6}s^3 + \frac{1}{24}s^4 - \frac{1}{120}s^5.$$

Each of these polynomials was truncated at its zero. For moderate times the differences are not significant, but the asymptotic results show greater deviations. For  $g_1(s)$ ,  $\alpha_S = 1$  for  $m = 1, 2, 3$ ; for  $g_3(s)$ ,  $\alpha_S$  takes the values 1.011, 1.007 and 0.986 for  $m = 1, 2$  and 3, respectively; and for  $g_5(s)$ ,  $\alpha_S$  takes the values 1.059, 1.130 and 1.183 (the values of  $I_n$  used to derive these are given in appendix B). For  $m = 1, 2$  these values are less than

those for Gaussian  $g(s)$ , and for  $m = 3$  they are positive, so that  $\alpha$  has a finite limit, unlike the Gaussian case.  $g_3(s)$  in 3 spatial dimensions shows that the closure does not ensure  $\alpha \geq 1$  in absolutely all cases—in this case the minimum value of  $\alpha$  is 0.96759 at a non-dimensional time of about 137. Mole *et al.* [15] consider the effects of non-Gaussian mean in more detail.

**5. – Discussion**

The model presented here has the advantage of being simple and computationally inexpensive. It is based on the exact eq. (3) for the concentration moments, together with the simple closure (5). Since the closure is applied within an integral over all space, one might expect the results to be more robust than for pointwise closures. Clarke and Mole [8] present experimental evidence in support of the use of the closure, and demonstrate that it satisfies some desirable properties for the parameter  $\alpha$ .

The model results for  $\alpha$  and  $\beta$  are in qualitative agreement with observation, but more detailed comparison is required. In general the evolution of  $\alpha$  and  $\beta$  in the model is completely determined by  $\mu_0, Q_1, Q_2, Q_3, \dot{Q}_2$  and  $\dot{Q}_3$ . Thus, if the experimental coverage is sufficient, the moments predicted by the model can be compared with observation by using the experimentally measured  $\mu(\mathbf{x}, t)$  to supply the above quantities. Extension of the model to realistic shear flows can be accomplished by incorporating appropriate models for the mean concentration.

For instantaneous releases (corresponding to  $m = 3$  in the model) the greater difficulty of obtaining appropriate data means that direct verification of the validity of (1) and (2) has not yet been attempted. Given the importance of such releases for practical hazard assessment, it is vital for the validation and development of this model that suitable data are obtained for this purpose. Some indirect support for the validity of (1) and (2) in this case has been provided by Heagy and Sullivan [16], and further such work is in progress by ourselves.

Finally, a simpler version of the models described here has been developed by Labropulu and Sullivan [17]. They make use of (3) for  $n = 2$  only, by making some further assumptions. Comparison between this model and ours is currently being carried out.

\* \* \*

We would like to thank P. CHATWIN and P. SULLIVAN for many helpful discussions. NM received funding from The Royal Society and Canada NSERC, EDC was supported by an EPSRC/HSE CASE Studentship, and ER was supported under the EU ERASMUS scheme.

APPENDIX A.

Schwarz's inequality (see, *e.g.*, 3.2.11 of Abramowitz and Stegun [18]) states that for two real functions  $f$  and  $g$

$$\left(\int fg\right)^2 \leq \left(\int f^2\right) \left(\int g^2\right),$$

with equality if and only if  $g$  is proportional to  $f$ . If we choose  $f = \mu^{1/2}$  and  $g = \mu^{3/2}$ , then we get

$$Q_2^2 \leq QQ_3,$$

with equality if and only if  $\mu^{1/2}$  is proportional to  $\mu^{3/2}$ , i.e.  $\mu$  is uniform throughout the cloud. Dividing through by  $\mu_0^2 Q^2$  gives

$$\hat{Q}_3 - \hat{Q}_2^2 \geq 0.$$

At large time we cannot have uniform mean concentration within a cloud in unbounded fluid, so the inequality is strict. Thus we must have

$$\hat{Q}_2 \hat{Q}_3 > \hat{Q}_2 (3\hat{Q}_2^2 - 2\hat{Q}_3).$$

If  $3\hat{Q}_2^2 - 2\hat{Q}_3 > 0$ , this gives  $\alpha_S > \hat{Q}_2$ , and if  $3\hat{Q}_2^2 - 2\hat{Q}_3 < 0$  it gives  $\alpha_S < -\hat{Q}_2$ .

#### APPENDIX B.

For  $g = g_1$  we have

$$I_n = \begin{cases} \frac{2^{2n+1}(n!)^2}{(2n+1)!}, & m = 1, \\ \frac{1}{n+1}, & m = 2, \\ \frac{2^{2n+2}n!(n+1)!}{(2n+3)!}, & m = 3. \end{cases}$$

For  $g = g_3$  the symbolic mathematical calculation package MAPLE was used to derive the following values:

$$I_1 = \begin{cases} 1.5815, & m = 1, \\ 0.7296, & m = 2, \\ 0.4871, & m = 3, \end{cases}$$

$$I_2 = \begin{cases} 1.2115, & m = 1, \\ 0.4500, & m = 2, \\ 0.2515, & m = 3, \end{cases}$$

$$I_3 = \begin{cases} 1.0096, & m = 1, \\ 0.3187, & m = 2, \\ 0.1543, & m = 3. \end{cases}$$

For  $g = g_5$  MAPLE was used to derive the following values:

$$I_1 = \begin{cases} 1.6807, & m = 1, \\ 0.8507, & m = 2, \\ 0.6368, & m = 3, \end{cases}$$

$$I_2 = \begin{cases} 1.2425, & m = 1, \\ 0.4846, & m = 2, \\ 0.2909, & m = 3, \end{cases}$$

$$I_3 = \begin{cases} 1.0213 & m = 1 \\ 0.3307 & m = 2 \\ 0.1671 & m = 3. \end{cases}$$

## REFERENCES

- [1] CHATWIN P. C. and SULLIVAN P. J., *J. Fluid Mech.*, **212** (1990) 533-556.
- [2] SULLIVAN P. J. and YIP H., in *Continuum Mechanics and its Applications*, edited by G. A. C. GRAHAM and S. K. MALIK (Hemispheric Publication Corp.) 1989, pp. 837-847.
- [3] CHATWIN P. C., SULLIVAN P. J. and YIP H., in *Proc. Int. Conference on Physical Modelling of Transport and Dispersion*, edited by E. E. ADAMS and G. E. HECKER (MIT), 1990, pp. 6B3-6B8.
- [4] MOSELEY D. J., M.Sc. dissertation (University of Western Ontario) 1991.
- [5] SAWFORD B. L. and SULLIVAN P. J., *J. Fluid Mech.*, **289** (1995) 141-157.
- [6] CHATWIN P. C. and SULLIVAN P. J., *Math. Comput. Simul.*, **32** (1990) 49-57.
- [7] MOLE N., *Environmetrics*, **6** (1995) 559-569.
- [8] CLARKE E. D. and MOLE N., *Environmetrics*, **6** (1995) 607-617.
- [9] BATCHELOR G. K., *Proc. Cambridge Philos. Soc.*, **48** (1952) 345-362.
- [10] BATCHELOR G. K., *Australian J. Sci. Res. Ser. A*, **2** (1949) 437-450.
- [11] BECKER H. A., HOTTEL H. C. and WILLIAMS G. C., *J. Fluid Mech.*, **30** (1967) 285-303.
- [12] BIRCH A. D., BROWN D. R., DODSON M. G. and THOMAS J. R., *J. Fluid Mech.*, **88** (1978) 431-449.
- [13] GAD-EL HAK M. and MORTON J. B., *AIAA J.*, **17** (1979) 558-562.
- [14] MOLE N. and CLARKE E. D., *Boundary-Layer Meteorol.*, **73** (1995) 35-52.
- [15] MOLE N., CLARKE E. D. and RIETZLER E., *Proc. MODSIM 95, International Congress on Modelling and Simulation*, Vol. 1 (1995) pp. 219-225.
- [16] HEAGY W. K. and SULLIVAN P. J., *Atmos. Environ.*, **30** (1996) 35-47.
- [17] LABROPULU F. and SULLIVAN P. J., *Environmetrics*, **6** (1995) 619-625.
- [18] ABRAMOWITZ M. and STEGUN I. A. (Editors), *Handbook of Mathematical Functions* (Dover, New York) 1964.